

Logits DeConfusion with CLIP for Few-Shot Learning

Shuo Li, Fang Liu*, Zehua Hao, Xinyi Wang, Lingling Li, Xu Liu, Puhua Chen, Wenping Ma
 Key Laboratory of Intelligent Perception and Image Understanding of Ministry of Education,
 International Research Center for Intelligent Perception and Computation,
 Joint International Research Laboratory of Intelligent Perception and Computation,
 School of Artificial Intelligence, Xidian University, Xi'an 710071, China

lishuo@xidian.edu.cn, f63liu@163.com

Abstract

With its powerful visual-language alignment capability, CLIP performs well in zero-shot and few-shot learning tasks. However, we found in experiments that CLIP’s logits suffer from serious inter-class confusion problems in downstream tasks, and the ambiguity between categories seriously affects the accuracy. To address this challenge, we propose a novel method called Logits DeConfusion, which effectively learns and eliminates inter-class confusion in logits by combining our Multi-level Adapter Fusion (MAF) module with our Inter-Class Deconfusion (ICD) module. Our MAF extracts features from different levels and fuses them uniformly to enhance feature representation. Our ICD learnably eliminates inter-class confusion in logits with a residual structure. Experimental results show that our method can significantly improve the classification performance and alleviate the inter-class confusion problem. The code is available at <https://github.com/LiShuo1001/LDC>.

1. Introduction

Recently, the outstanding performance of Vision-Language Models (VLMs) [68] in visual understanding has attracted widespread attention [36]. CLIP (Contrastive Language-Image Pretraining) [48], as a representative model, successfully maps images and texts to a common embedding space through large-scale image-text contrastive learning, and achieves Zero-Shot Learning (ZSL) on unseen categories, thereby reducing the dependence on labeled data and demonstrating excellent transfer learning capabilities [65]. In Few-Shot Learning (FSL), the goal is to quickly adapt to classification tasks of new categories with very few labeled training samples [67]. CLIP shows unique advantages in such tasks, and its pre-trained rich features help improve the generalization ability of the model [23]. However, although

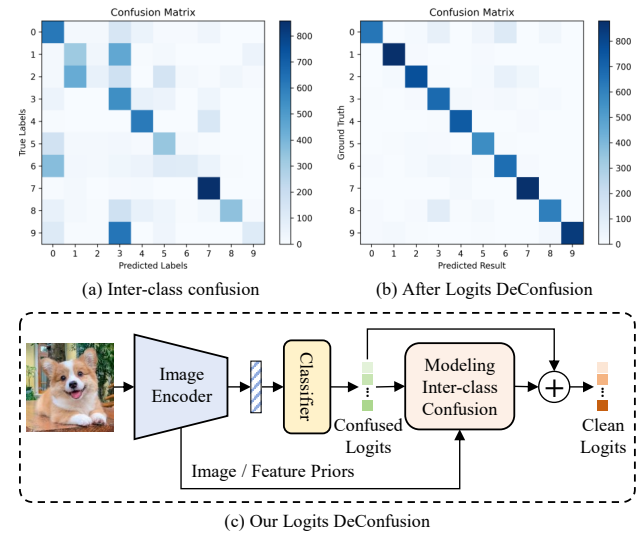


Figure 1. (a) Inter-class confusion of logits in CLIP-based ZSL. (b) After remove inter-class confusion of logits. (c) Our Logits DeConfusion models inter-class confusion and removes it.

CLIP-based FSL has great potential [51, 70], its logits often show serious inter-class confusion, resulting in a decrease in classification accuracy, which limits the performance improvement of applying CLIP to FSL [35].

In the original CLIP-based ZSL [48] experiment, as shown in Figure 1 (a), we found that its logits have significant inter-class confusion, which is manifested as the difficulty in accurately distinguishing the predicted values of different categories in downstream tasks. The main reason for this phenomenon is the *pre-training strategy of CLIP*. CLIP is pre-trained on large-scale image-text pairs via contrast learning, rather than directly optimizing the classification boundaries [48]. Therefore, the ability to distinguish categories in classification tasks is insufficient, which leads to obvious inter-class confusion in logits. In addition, the *significant domain differences between the down-*

*Corresponding author

stream data and the CLIP pre-training data further exacerbate the confusion between logits of different categories. This inter-class confusion has a serious negative impact on CLIP-based FSL, and it is difficult for the model to learn a reliable classifier from a small number of samples. Especially when the similarity between categories is high, the inter-class confusion problem will be further exacerbated. Therefore, *how to effectively eliminate the inter-class confusion and improve the performance of CLIP-based FSL has become an important challenge that needs to be solved.*

To address the above challenge in CLIP-based FSL [57, 63], we propose to *model and eliminate inter-class confusion through learning*. Specifically, we first use a small number of samples to model inter-class confusion through a learnable module, which aims to capture inter-class confusion pattern from CLIP’s logit using image features as prior information, and then eliminate these confusions through a residual structure to obtain new logits with less confusion. The advantage of modeling and eliminating inter-class confusion is that it can not only *adaptively learn the confusion pattern between classes*, but also *eliminate this confusion through a residual structure*, thereby making the model have stronger generalization ability and accuracy.

In our work, based on the above motivation, as shown in Figure 1 (c), we propose a method called Logits DeConfusion (LDC), which includes a Multi-level Adapter Fusion (MAF) module and an Inter-Class Deconfusion (ICD) module. First, the MAF module extracts and fuses features from different levels of the CLIP image encoder to construct a unified feature representation, thereby improving adaptability to FSL tasks. Second, the ICD module introduces visual features to provide prior guidance on inter-class confusion, and learns the inter-class confusion patterns through a learnable module, and then removes them through a residual structure to obtain clearer category distinction. As shown in Figure 1 (b), our method can not only effectively alleviate the inter-class confusion problem and improve classification performance, but also retain the rich feature expression of CLIP and enhance its generalization ability and robustness. In summary, our main contributions are as follows:

- A novel Logits DeConfusion method is proposed, which combines a multi-level adapter fusion module and an inter-class deconfusion module to alleviate the inter-class confusion of CLIP-based FSL through learning.
- A multi-level adapter fusion module is designed, which extract and fuse features from different levels of the CLIP image encoder to enhance the image feature representation ability of our method.
- Our proposed inter-class deconfusion module effectively models and eliminates inter-class confusion patterns from visual features and CLIP logits through a learnable module with residuals, improving the ability to distinguish categories in downstream FSL tasks.

- Experimental results on multiple benchmarks demonstrate that our method significantly improves the classification performance and exhibits stronger generalization.

2. Related Work

In this section, we mainly introduce related work from the following two aspects: Zero/Few-shot Learning (Section 2.1) and CLIP-based Zero/Few-shot Learning (Section 2.2).

2.1. Zero/Few-shot Learning

Zero-Shot Learning (ZSL) and Few-Shot Learning (FSL) are important methods proposed in the field of machine learning to deal with insufficient labeled data [45]. In ZSL, the model needs to classify unseen categories without any labeled data during training [64]. To address this challenge, early methods often rely on semantic embeddings (such as word embeddings [69] or attribute features) to transfer knowledge from known categories to unseen categories [50]. In addition, Generative Adversarial Networks (GANs) and Variational AutoEncoders (VAEs) have been introduced into the field of ZSL to improve classification capabilities by generating virtual samples of unseen categories [59]. Although these methods have improved generalization capabilities to a certain extent, they often rely on accurate semantic representations and labeling information, which makes it difficult to generalize in complex scenarios [53]. In FSL, models that can quickly adapt to new tasks are designed to solve learning problems with only a small number of labeled samples [7, 30]. Meta-learning is a classic method in FSL that simulates few-shot scenarios in the training phase so that the model can efficiently adapt to new categories of learning tasks in the testing phase [55]. In addition, metric learning methods [24] learn a metric space suitable for few-shot tasks so that samples of new categories are well distinguishable in this space. Although FSL has made progress in tasks such as classification [18, 25] and detection [20], it still has the problem of insufficient generalization ability when faced with high similarity between categories [3] or large domain differences [71].

2.2. CLIP-based Zero/Few-shot Learning

The introduction of CLIP brings breakthrough progress to ZSL and FSL [16, 48]. In ZSL, CLIP can achieve direct classification without labeled data by comparing images with natural language descriptions of categories [56, 74]. This property has enabled CLIP to achieve significant performance improvements on multiple datasets and has triggered a large number of follow-up studies on cross-modal representation learning [29, 46]. Some subsequent methods such as CoOp (Context Optimization) [73] and CoCoOp (Conditional CoOp) [72] have further improved the adaptability of CLIP in different tasks by introducing learnable prompts [15]. However, although CLIP performs well

in ZSL, it is easy to cause confusion between categories in downstream tasks because it does not directly optimize the classification boundaries during the pre-training process [26, 62]. Recently, CLIP-based FSL has received widespread attention [52, 57]. Studies have shown that CLIP can improve classification performance in FSL tasks through its rich visual representation and cross-modal learning capabilities [28, 40, 51]. Many methods adaptively adjust CLIP through prompt-learning [37, 38, 61], fine-tuning [33, 63, 70], and other techniques [17, 31] to enhance its generalization ability in FSL tasks [1]. For example, Tip-Adapter [70] introduces an adapter that enables CLIP to quickly adapt to new tasks and achieve good performance in FSL scenarios. However, although these methods improve the adaptability of CLIP-based FSL, the inter-class confusion problem in new tasks still exists.

3. Our Approach

Our method aims to explore the transferability of CLIP with few samples so that it can be applied to new domains.

3.1. Problem Statement

In our work, we focus on using CLIP for downstream image classification tasks in the FSL setting [48, 57]. Given a training set $\mathcal{D}_{train} = \{(x_i, y_i)\}_{i=1}^{C \times K}$, where x_i is an image and $y_i \in \{1, 2, \dots, C\}$ is the label of the image x_i . In the training set, there are K images for each class, so there are a total of $C \times K$ images for training. Our work can be simply viewed as an efficient parameter fine-tuning CLIP using $C \times K$ training images, with the goal of learning learnable parameters θ by minimizing the loss function \mathcal{L} :

$$\mathcal{L}(\theta) = -\frac{1}{C \times K} \sum_{i=1}^K \sum_{\bar{y}=1}^C \log P(\bar{y}|x_i; \theta), \quad (1)$$

where $P(\bar{y}|x_i; \theta)$ is the probability that the model predicts that the image x_i belongs to the class \bar{y} . To evaluate the performance of the model, a test set $\mathcal{D}_{test} = \{(x_j, y_j)\}_{j=1}^N$ is given, where x_j is an image and $y_j \in \{1, 2, \dots, C\}$ is the label of the image x_j , N is the total number of test images. For each image x_j in the test set, we use the fine-tuned model to make classification predictions:

$$\hat{y}_j = \arg \max_{\bar{y} \in \{1, 2, \dots, C\}} P(\bar{y}|x_j; \theta), \quad (2)$$

and calculate the accuracy ACC on the test set:

$$ACC = \frac{1}{N} \sum_{j=1}^N \mathbb{I}(\hat{y}_j = y_j), \quad (3)$$

where $\mathbb{I}(\cdot)$ is an indicator function, which takes the value of 1 when the prediction \hat{y}_j is equal to the label y_j and 0 otherwise. Note that in the setting of this work, the test set contains the same C categories as the training set.

3.2. CLIP and Modeling Logits DeConfusion

In this work, our model is built on CLIP, which achieves ZSL by establishing a shared embedding space between images and text through contrastive learning [48]. Given a test image x_i and a set of text prompts $\mathcal{T} = \{t_1, t_2, \dots, t_C\}$ representing C categories, CLIP predicts the zero-shot logits s_i^{ZS} and the category \hat{y}_i of the image x_i . Specifically, CLIP first calculates the cosine similarity $s(x_i, t_{\bar{y}_i})$ of each image-text pair $(x_i, t_{\bar{y}_i})$, then normalizes it using softmax to get the zero-shot logit $s_i^{ZS}[\bar{y}_i]$, and finally predicts the category \hat{y}_i corresponding to the maximum zero-shot logit:

$$\begin{aligned} \hat{y}_i &= \arg \max_{\bar{y}_i \in \{1, 2, \dots, C\}} s_i^{ZS}[\bar{y}_i], \\ s_i^{ZS}[\bar{y}_i] &= \frac{\exp(s(x_i, t_{\bar{y}_i}))}{\sum_{\bar{y}'_i \in \{1, 2, \dots, C\}} \exp(s(x_i, t_{\bar{y}'_i}))} \\ s(x_i, t_{\bar{y}_i}) &= \frac{z_{x_i} \cdot z_{t_{\bar{y}_i}}}{\|z_{x_i}\| \|z_{t_{\bar{y}_i}}\|} \end{aligned} \quad (4)$$

where $z_{x_i} = \mathcal{E}_I(x_i)$ and $z_{t_{\bar{y}_i}} = \mathcal{E}_T(t_{\bar{y}_i})$ are the embeddings of the image and text respectively, and \cdot represents the cosine similarity. Through this process, CLIP is able to make predictions for new categories without additional training by simply adding their text prompts to \mathcal{T} [73].

Although CLIP has strong zero-shot capabilities, it is difficult to capture fine-grained features related to downstream tasks due to the pre-training method and data distribution, resulting in serious inter-class confusion in the predicted zero-shot logits s_i^{ZS} . In the experiment, we also found that there are some fixed inter-class confusion patterns for each category in s_i^{ZS} . To alleviate this phenomenon, we directly model and learn these patterns in logits and hope to remove them with the idea of residual learning. Specifically, we first assume that the inter-class confusion in logits can be represented as an additional noise term Δs :

$$\hat{s}_i = s_i^{ZS} - \Delta s(x_i), \quad (5)$$

where \hat{s}_i is the clean logits and $\Delta s(x_i)$ model the inter-class confusion of the image x_i . Then, we learn the additional noise term $\Delta s(x_i)$ through a learnable module \mathcal{E}_Δ :

$$\Delta s(x_i) = \mathcal{E}_\Delta(s_i^{ZS}, x_i). \quad (6)$$

The learnable module \mathcal{E}_Δ takes the image x_i as prior and learns the inter-class confusion pattern from zero-shot logits s_i^{ZS} . In this way, the learnable parameters in our method can be optimized by minimizing the cross entropy loss between the clean logits \hat{s}_i and the label y_i :

$$\mathcal{L}_{CE}(\hat{s}_i, y_i) = -\log \hat{s}_i[y_i]. \quad (7)$$

To prevent over-deconfusion, we adopt a similarity loss \mathcal{L}_{sim} with L_1 regularization to ensure that the clean logits \hat{s}_i and the original zero-shot logits s_i^{ZS} maintain similar:

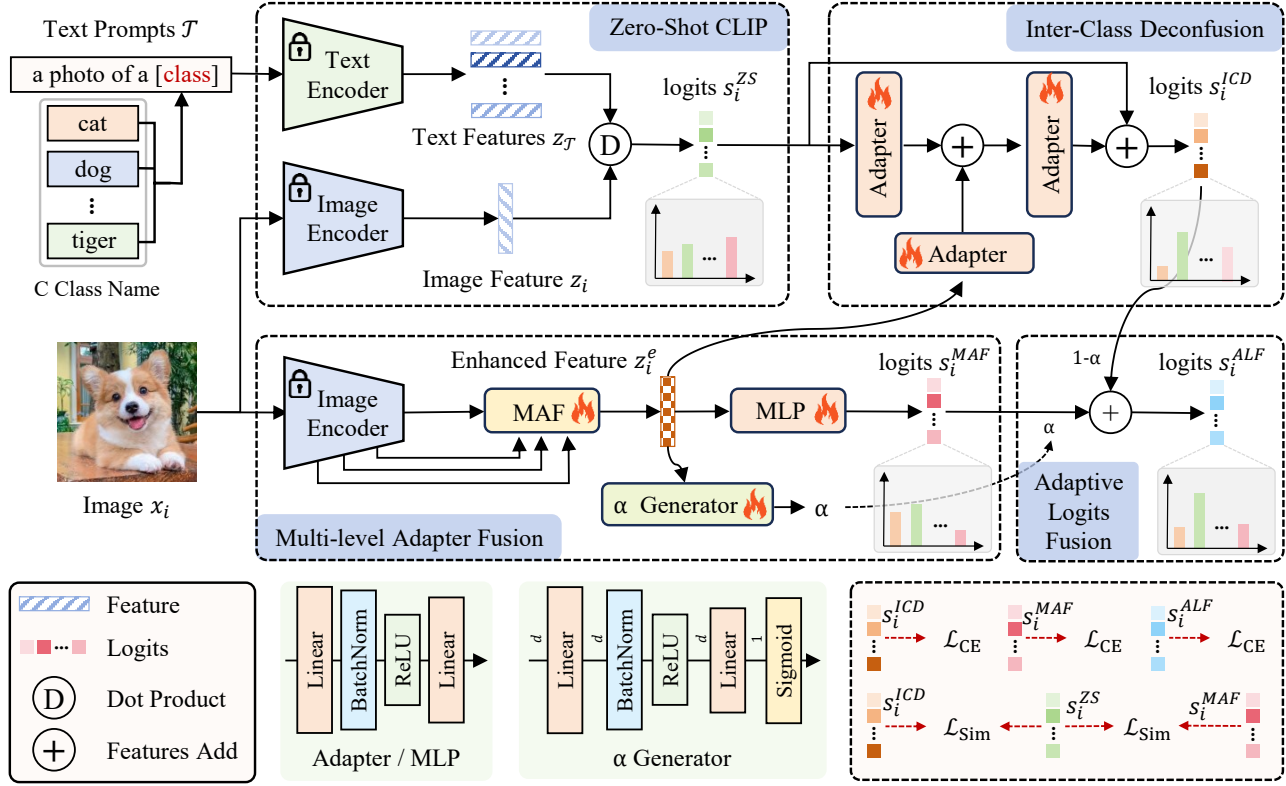


Figure 2. Overall architecture of our LDC. Our method consists of four main modules, namely Zero-Shot CLIP (ZS-CLIP), Inter-Class Deconfusion (ICD), Multi-level Adapter Fusion (MAF), and Adaptive Logits Fusion (ALF). In addition, our method includes three cross-entropy losses and two similarity losses for optimizing the learnable parameters. In ALF, the α Generator generates an adaptive weight α used to fuse the logits s_i^{MAF} and s_i^{ICD} . All learnable parameters are in ICD, MAF, and α Generator. MAF is detailed in Section 3.4.

$$\mathcal{L}_{sim}(\hat{s}_i, s_i^{ZS}) = \|\hat{s}_i - s_i^{ZS}\|_1. \quad (8)$$

Finally, the total loss for modeling Logits DeConfusion is:

$$\mathcal{L} = \mathcal{L}_{CE}(\hat{s}_i, y_i) + \lambda \mathcal{L}_{sim}(\hat{s}_i, s_i^{ZS}), \quad (9)$$

where λ is a trade-off parameter used to balance the impact between the cross entropy loss and the similarity loss.

3.3. Method Overview

The overall architecture of our method is shown in Figure 2, which consists of four main modules: Zero-Shot CLIP (ZS-CLIP), Multi-level Adapter Fusion (MAF), Inter-Class Deconfusion (ICD), and Adaptive Logits Fusion (ALF).

First, we obtain the zero-shot logits s_i^{ZS} of the original ZS-CLIP through Eq. 4. Then, through the MAF module, we transform and fuse the features of different levels of the image encoder \mathcal{E}_I into an enhanced feature z_i^e , which integrates low-level detail information and high-level semantic information, making it more generalizable when faced with few annotated training images. After an MLP, we get

the MAF logits s_i^{MAF} with only the visual feature as input. Next, the ICD module uses the enhanced feature z_i^e as priors and learns inter-class confusion from the zero-shot logits s_i^{ZS} through a residual structure. Finally, in ALF, the MAF logits s_i^{MAF} and the ICD logits s_i^{ICD} are fused in a learning manner to obtain the final ALF logits s_i^{ALF} , where the adaptive fusion weight α is generated by a α Generator. To optimize learnable parameters in ICD, MAF, and α Generator, we use multiple losses to jointly learn, such as the cross entropy loss \mathcal{L}_{CE} between the MAF logits s_i^{MAF} and the label y_i , the similarity loss \mathcal{L}_{Sim} between the MAF logits s_i^{MAF} and the zero-shot logits s_i^{ZS} , etc.

3.4. Multi-level Adapter Fusion

Our proposed MAF module aims to fully exploit the diversity of features at each level of the image encoder \mathcal{E}_I . By transforming and fusing features at different levels, our MAF module not only retains the detailed information of low-level features, but also effectively utilizes the abstract semantic information of high-level features. Specifically, as shown in Figure 3, our MAF contains multiple side Adapters, a Fusion mechanism, and a Projector. First, four

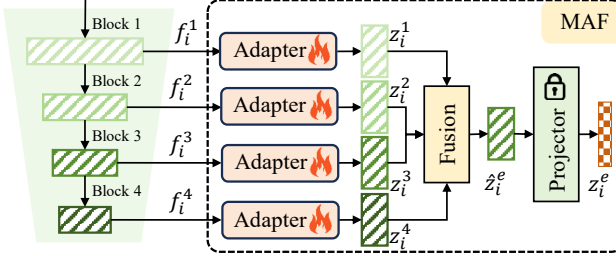


Figure 3. Details of MAF. On the left is the image encoder \mathcal{E}_I .

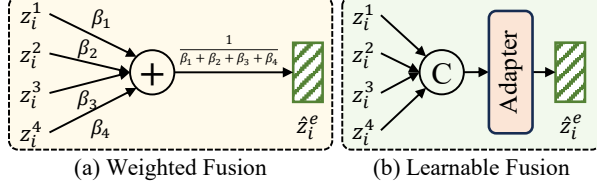


Figure 4. Details of our Fusion mechanisms.

different levels of features f_i^1, f_i^2, f_i^3 , and f_i^4 are obtained from the image encoder \mathcal{E}_I . Then, these four features are transformed through different Adapters to obtain four new features z_i^1, z_i^2, z_i^3 , and z_i^4 . Next, these features are fused into one fused feature \hat{z}_i^e through our Fusion mechanism. Finally, an enhanced feature z_i^e is obtained through the frozen Projector. It is worth noting that when the image encoder is based on the ResNet architecture, the Projector is an attention pooling layer, and when the image encoder is based on ViT, the Projector is a linear projection layer.

In our MAF, we propose two different Fusion mechanisms: Weighted Fusion (WF) and Learnable Fusion (LF). As shown in Figure 4 (a), WF first fuses features of different levels through preset weights $\beta_1, \beta_2, \beta_3$, and β_4 , and then get the fused feature \hat{z}_i^e by dividing $\beta_1 + \beta_2 + \beta_3 + \beta_4$. As shown in Figure 4 (b), LF first concatenates features across the feature channel dimension and then uses an Adapter to reduce the dimension to obtain the fused feature \hat{z}_i^e , where the detailed structure of the Adapter is shown in Figure 2.

3.5. Inter-Class Deconfusion

In order to solve the inter-class confusion phenomenon that occurs when CLIP is applied to downstream tasks, we propose an Inter-Class Deconfusion (ICD) module that uses a residual structure to learn and alleviate inter-class confusion in the zero-shot logits s_i^{ZS} . Specifically, first, an Adapter \mathcal{E}_{A1}^{ICD} learns the inter-class confusion pattern from the zero-shot logits s_i^{ZS} , then another Adapter \mathcal{E}_{A2}^{ICD} learns the prior of inter-class confusion from the enhanced feature z_i^e , then the outputs of \mathcal{E}_{A1}^{ICD} and \mathcal{E}_{A2}^{ICD} are sent to the third Adapter \mathcal{E}_{A3}^{ICD} to jointly learn the inter-class confusion pattern from the zero-shot logits s_i^{ZS} and the enhanced feature z_i^e , and finally the residual structure is used to remove the learned

inter-class confusion pattern to obtain a relatively clean ICD logits s_i^{ICD} . The above process can be expressed as:

$$\begin{aligned} s_i^{ICD} &= s_i^{ZS} - \mathcal{E}_\Delta(s_i^{ZS}, z_i^e) \\ &= s_i^{ZS} + \mathcal{E}_{A3}^{ICD}(\mathcal{E}_{A1}^{ICD}(s_i^{ZS}) + \mathcal{E}_{A2}^{ICD}(z_i^e)). \end{aligned} \quad (10)$$

Our ICD module not only takes into account the confusion cues of the zero-shot logits s_i^{ZS} itself, but also introduces the enhanced feature z_i^e to give cues of inter-class confusion. In this way, our ICD module learns the inter-class confusion patterns and weakens such patterns in the form of residuals, making better use of the knowledge learned from CLIP and improving the modeling ability of new domain data, especially in the FSL setting.

3.6. Adaptive Logits Fusion

After obtaining the ICD logits s_i^{ICD} from the ICD module, we further propose an Adaptive Logits Fusion (ALF) module, which fuses the ICD logits s_i^{ICD} with the MAF logits s_i^{MAF} in an adaptive manner to obtain the final ALF logits s_i^{ALF} . Specifically, we first design a α Generator that generates an adaptive weight α using the enhanced feature z_i^e , and then use the adaptive weight α to weightedly fuse the ICD logits s_i^{ICD} and the MAF logits s_i^{MAF} :

$$s_i^{ALF} = \alpha s_i^{MAF} + (1 - \alpha) s_i^{ICD}, \quad \alpha = \mathcal{E}_{G_\alpha}(z_i^e), \quad (11)$$

where \mathcal{E}_{G_α} is the α Generator, as shown in Figure 2.

Through the above ALF module, our method can adaptively combine inter-class confusion with multi-level features, making the final ALF logits s_i^{ALF} more robust and accurate. The core of this is to use the adaptive weight α to adaptively adjust the weight between the ICD logits and the MAF logits to ensure a more reasonable fusion.

3.7. Training Objective

In the optimization stage, we use the cross-entropy loss (\mathcal{L}_{CE}) and the L_1 similarity loss (\mathcal{L}_{Sim}) to jointly optimize the learnable parameters of our method. Specifically, we use Eq. 7 to calculate the loss \mathcal{L}_{CE}^{MAF} between s_i^{MAF} and y_i , the loss \mathcal{L}_{CE}^{ICD} between s_i^{ICD} and y_i , and the loss \mathcal{L}_{CE}^{ALF} between s_i^{ALF} and y_i to ensure the classification accuracy:

$$\begin{aligned} \mathcal{L}_{CE} &= \mathcal{L}_{CE}^{MAF}(s_i^{MAF}, y_i) + \\ &\quad \mathcal{L}_{CE}^{ICD}(s_i^{ICD}, y_i) + \mathcal{L}_{CE}^{ALF}(s_i^{ALF}, y_i). \end{aligned} \quad (12)$$

In addition, in order to avoid over-deconfusion, we keep the similarity between the output logits and the original zero-shot logits. Specifically, we use Eq. 8 to calculate the similarity loss \mathcal{L}_{Sim}^{MAF} between s_i^{MAF} and s_i^{ZS} and the similarity loss \mathcal{L}_{Sim}^{ICD} between s_i^{ICD} and s_i^{ZS} :

$$\mathcal{L}_{Sim} = \mathcal{L}_{Sim}^{MAF} + \mathcal{L}_{Sim}^{ICD}. \quad (13)$$

Finally, as shown in Eq. 9, the total loss \mathcal{L} is:

$$\mathcal{L} = \mathcal{L}_{CE} + \lambda \mathcal{L}_{Sim}. \quad (14)$$

where λ is a trade-off parameter.

4. Experimental Results

In this section, we conduct extensive experiments to verify the effectiveness of the proposed method and illustrate the contribution of each module to the performance.

4.1. Datasets

To validate our method, we consider 11 image classification benchmarks: ImageNet [5], Caltech101 [8], DTD [4], EuroSAT [13], FGVC Aircraft [34], Flowers102 [39], Food101 [2], OxfordPets [42], StanfordCars [21], SUN397 [66], and UCF101 [54]. In addition, in order to verify the generalization ability, we use ImageNet [5] as training data and ImageNet-Sketch [60] and ImageNet-V2 [49] benchmarks as out-of-domain distributions (OOD). We follow the FSL setting of CLIP [48] and use 1, 2, 4, 8, and 16 images per class to train our model and evaluate the results on the test set. Following the data splitting strategy of previous methods, such as CoOp [73] and Tip-Adapter [70], we divide each dataset into training, validation, and test sets.

4.2. Implementation Details

For fair comparison, our experiments are performed on ResNet-50 [12] unless otherwise specified. We train all tasks for 50 epochs and use AdamW [41] with an initial learning rate of 0.001 and a batch size of 64. The input size of all datasets is 224, and random resized crop and horizontal flip are used as augmentation methods. In WF, β_1 , β_2 , β_3 , and β_4 are set to 0.1, 0.2, 0.3, and 0.4, respectively. In the loss, the value of λ is 1.0. All experiments are implemented based on PyTorch [43] and performed on a single NVIDIA GTX 4090D GPU. The training and testing time on all datasets for the 16-shot setting is about 37 minutes.

4.3. Comparison with the State-of-the-art

The effectiveness of our method is evaluated in two settings: downstream classification benchmarks and OOD data.

4.3.1. Results on Classification Benchmarks

To verify the effectiveness of our LDC, we compare it with several SOTA CLIP-based FSL methods with ResNet-50 [12] as the backbone on ImageNet [5], such as CoOp [73], VT-CLIP [47], Tip-Adapter [70], SuS-X [58], FAR [63], CALIP-FS [11], SGVA-CLIP [44], Proto-CLIP-F [40], APE [75], DAC-V [10], and LP++ [14]. Experimental results are shown in Table 1. It can be seen that our method has achieved the best accuracy in some cases. For example, in the 16-shot setting, we achieve an accuracy of 66.63%,

Method	K-Shot Accuracy (%)				
	1	2	4	8	16
LP-CLIP [48]	22.17	31.90	41.20	49.52	56.13
CoOp [73]	57.15	57.81	59.99	61.56	62.95
VT-CLIP [47]	60.53	61.29	62.02	62.81	63.92
Tip-Adapter [70]	60.70	60.92	60.95	61.48	62.00
Tip-Adapter-F [70]	61.32	61.69	62.52	64.00	65.51
SuS-X [58]	60.73	61.03	61.10	61.57	62.16
FAR [63]	60.80	61.90	62.40	64.30	66.39
CALIP-FS [11]	61.35	62.03	63.13	64.11	65.81
SGVA-CLIP [44]	61.00	62.70	63.10	64.20	65.70
Proto-CLIP-F [40]	60.32	60.64	61.30	63.92	65.75
APE [75]	62.04	62.34	62.54	62.79	63.42
CLIP-Adapter [9]	61.20	61.52	61.84	62.68	63.59
DAC-V [10]	60.71	61.48	61.87	63.38	64.89
LP++ [14]	61.20	61.60	62.60	63.80	64.70
LDC (Our)	60.48	61.25	62.47	64.44	66.63
	-1.56	-1.45	-0.66	+0.14	+0.24

Table 1. Comparison of different methods on ImageNet.

Method	K-Shot Accuracy (%)					
	0	1	2	4	8	16
ZS-CLIP	58.87	-	-	-	-	-
LP-CLIP [48]	-	36.67	47.61	57.19	64.98	71.10
CoOp [73]	-	59.80	62.21	66.84	70.05	73.45
Tip-Adapter [70]	-	62.32	64.64	66.51	68.41	70.36
Tip-Adapter-F [70]	-	64.55	66.79	69.76	72.59	75.69
SuS-X [58]	-	62.87	65.29	67.64	69.37	71.36
APE [75]	-	65.13	67.19	69.47	71.58	73.36
CLIP-Adapter [9]	-	62.90	65.11	68.02	71.52	74.50
Proto-CLIP [40]	-	62.83	66.04	68.19	70.01	71.57
Proto-CLIP-F [40]	-	61.84	65.96	68.29	73.13	76.18
LDC (Our)	-	65.71	67.92	71.17	75.79	79.78
	-	+0.58	+0.73	+1.41	+2.66	+3.60

Table 2. Comparison of different methods over 11 datasets.

which is 0.24 higher than the previous best method. To comprehensively evaluate our method on a variety of downstream tasks, we summarize the average FSL classification performance of various methods with 1, 2, 4, 8, and 16-shot settings on 11 datasets in Table 2. Overall, our method is the best on all settings, especially on the 16-shot setting, where we achieve an overall accuracy of 79.78%. These results show that our LDC can effectively model and learn inter-class confusion patterns and remove them. In addition, Figure 5 shows the detailed accuracy of our method and various comparison methods on 11 datasets, where the last one shows the average performance on these 11 datasets. It can be seen that the results of our method are excellent in most cases, especially on the EuroSAT [13], FGVC Aircraft [34], StanfordCars [21], and UCF101 [54] datasets.

4.3.2. Robustness to OOD Data

To verify the robustness of our method, we first train our model on ImageNet [5] in a 16-shot setting, and then test it

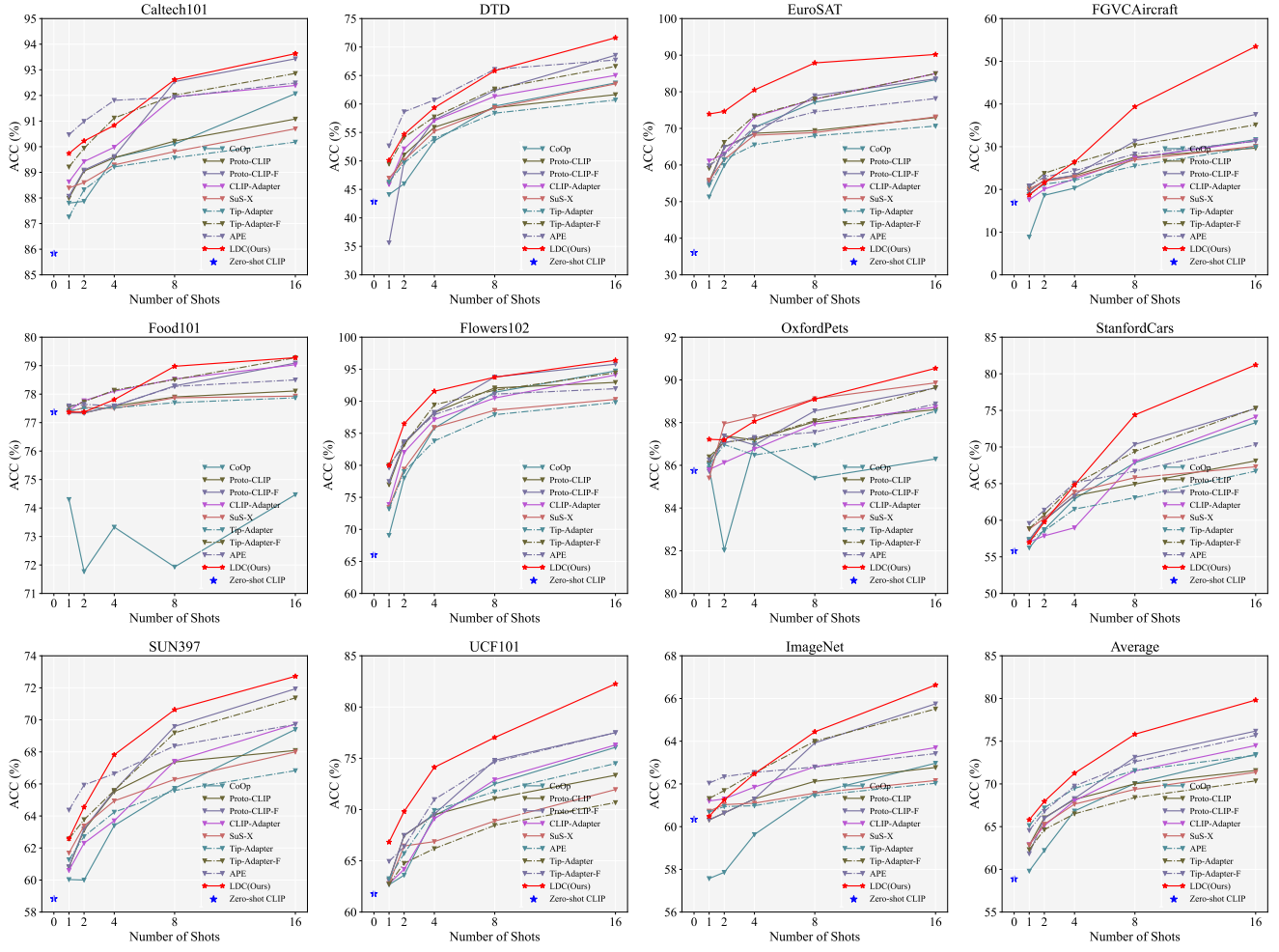


Figure 5. Classification performance of different methods on 11 datasets, and the last one is the average performance on these 11 datasets.

on ImageNet-V2 (V2) [49] and ImageNet-Sketch (Sketch) [60] to evaluate the performance of our method under OOD setting. Table 3 shows the performance of our method and other methods under two backbones, ResNet-50 [12] and ViT-B/16 [6]. It can be seen that our method performs well on ImageNet-V2 with both backbones, which confirms the robustness and transferability of our LDC. However, the performance on ImageNet-Sketch is not as expected, which indicates that our method may not be well suited for tasks with large domain differences and needs further study.

4.4. Ablation Experiment

To analyze the effect of our modules and settings, we conduct a series of ablation experiments over 11 datasets.

4.4.1. Effect analysis of each module

In our work, we mainly propose three modules, MAF, ICD, and ALF. To explore their respective roles, we perform a set of module ablation experiments under multiple backbones.

The experimental results are shown in Table 4. As can be seen from the table, our ICD significantly improves the average accuracy by 19.07% with ResNet50 [12] as the backbone and 16.46% with ViT-B/16 [6] as the backbone, which shows that our method can learn the inter-class confusion patterns and remove them, thus achieving our motivation.

4.4.2. Ablation study of MAF

The ablation results of our MAF module are shown in Table 5, including the ablation of multi-level features, fusion mechanisms, and projector. From the left of Table 5, it can be seen that as the number of feature levels increases, the average performance improves, which is consistent with intuition and previous experience [27, 32]. In the left of Table 5, "WF (0.25)" indicates $\beta_1=\beta_2=\beta_3=\beta_4=0.25$, and "WF (0.1/0.2/0.3/0.4)" indicates $\beta_1=0.1$, $\beta_2=0.2$, $\beta_3=0.3$, and $\beta_4=0.4$. From the results, we can observe that among our proposed fusion mechanisms, "WF (0.1/0.2/0.3/0.4)" achieves the best results. In addition, after fusion, the pro-

Method	Source	Target	
	ImageNet	V2	Sketch
ResNet-50	ZS-CLIP [48]	60.33	53.27
	LP-CLIP [48]	56.13	45.61
	CoOp [73]	62.95	54.58
	CoCoOp [72]	62.81	55.72
	CALIP-FS [11]	65.81	55.98
	CLIP-Adapter [9]	63.59	55.69
	APE [75]	63.42	55.94
	APE-T [75]	66.07	57.59
	Tip-Adapter [70]	62.03	54.60
	Tip-Adapter-F [70]	65.51	57.11
	DAC-V [10]	64.89	56.56
	DAC-VT [10]	66.61	57.68
	FAR [63]	66.39	57.91
	LDC (Our)	66.63 <small>+0.02</small>	58.03 <small>+0.12</small>
ViT-B/16	ZS-CLIP [48]	66.73	60.83
	CoOp [73]	71.51	64.20
	CoCoOp [72]	71.02	64.07
	MaPLe [19]	70.72	64.07
	RPO [22]	71.67	65.13
LDC (Our)	73.88 <small>+2.21</small>	66.10 <small>+0.97</small>	
	48.85 <small>-0.42</small>		

Table 3. Comparison of different methods under OOD setting.

Module	Backbone				
	MAF	ICD	ALF	ResNet50	ViT-B/16
✓				58.87	65.52
	✓			70.83 <small>+11.96</small>	74.57 <small>+9.05</small>
		✓		77.94 <small>+19.07</small>	81.98 <small>+16.46</small>
✓	✓			78.82 <small>+19.95</small>	82.41 <small>+16.89</small>
✓	✓	✓		79.78 <small>+20.91</small>	82.87 <small>+17.35</small>

Table 4. Effect analysis of each module over 11 datasets.

f_1	f_2	f_3	f_4	ACC	w/ or w/o	ACC
		✓		75.95	w/ WF (0.25)	79.71
	✓	✓		77.48	w/ WF (0.1/0.2/0.3/0.4)	79.78
✓	✓	✓	✓	79.10	w/ LF	79.59
✓	✓	✓	✓	79.78	w/o Projector	78.94

Table 5. Ablation study of MAF over 11 datasets.

jector also plays an important role in the performance.

4.4.3. Ablation study of ICD

The ablation experimental results of ICD are shown in Table 6, where " A_1 " means $\mathcal{E}_{A_1}^{ICD}(s_i^{ZS})$, " A_2 " means $\mathcal{E}_{A_2}^{ICD}(z_i^e)$, " A_3 " means $\mathcal{E}_{A_3}^{ICD}(\cdot)$, and "Res" means the residual structure. It can be seen that using the enhanced feature z_i^e as prior can improve the average performance. In addition, it can be seen from the last two rows that the residual structure can improve the performance by 1.24%.

4.4.4. Ablation study of ALF

The ablation experimental results of ALF are shown in Table 7, where α is generated by the α Generator. Compared to manually setting α to 0.5 in the 4-th row, our adaptive logits fusion improves by 0.54%. It also can be seen that

A_1	A_2	A_3	Res	ACC	ALF logits	ACC
✓		✓	✓	78.02	s_i^{ICD}	78.71
		✓	✓	79.36	s_i^{MAF}	77.35
✓	✓		✓	79.12	$s_i^{ICD} + s_i^{MAF}$	78.69
✓	✓	✓	✓	78.54	$(s_i^{ICD} + s_i^{MAF})/2$	79.24
✓	✓	✓	✓	79.78	$\alpha s_i^{ICD} + (1 - \alpha)s_i^{MAF}$	79.78

Table 6. ICD ablation.

Table 7. ALF logits ablation.

\mathcal{L}_{CE}^{MAF}	\mathcal{L}_{CE}^{ICD}	\mathcal{L}_{CE}^{ALF}	\mathcal{L}_{Sim}^{MAF}	\mathcal{L}_{Sim}^{ICD}	ACC
✓	✓				79.03
	✓	✓			75.47
✓	✓	✓			79.13
✓	✓	✓	✓		79.29
✓	✓	✓	✓	✓	79.43
✓	✓	✓	✓	✓	79.78

Table 8. Ablation study of training losses over 11 datasets.

fusing s_i^{ICD} and s_i^{MAF} can improve the average accuracy, regardless of whether the fusion weight is fixed or adaptive.

4.4.5. Ablation study of Training Losses

Our method contains multiple losses: three cross entropy losses for classification and two similarity losses to avoid over-deconfusion. Table 8 shows a set of ablation experiments on the losses. As can be seen from the table, similarity losses \mathcal{L}_{Sim}^{MAF} and \mathcal{L}_{Sim}^{ICD} play an important role.

5. Conclusion

This work proposes a novel Logits DeConfusion method to solve the inter-class confusion problem in CLIP-based few-shot learning tasks. Through the joint design of the Multi-level Adapter Fusion (MAF) module and the Inter-class Deconfusion (ICD) module, we effectively alleviate the inter-class confusion caused by the lack of clear classification boundaries during CLIP pre-training. The MAF module enhances the adaptability of image representation by extracting and fusing features from different levels, while the ICD module learns inter-class confusion through a learnable module with residuals, improving the clarity and accuracy of classification logits. Experimental results show that the proposed method significantly improves the classification accuracy on multiple benchmarks, verifying its effectiveness in dealing with inter-class confusion.

Acknowledgement: This work was supported Postdoctoral Fellowship Program of China Postdoctoral Science Foundation (CPSF) (GZC20232033), National Natural Science Foundation of China (62406231), China Postdoctoral Science Foundation (2023M742738), Shaanxi Province Postdoctoral Research Project Funding (2024BSHSDZZ119), Joint Fund Project of National Natural Science Foundation of China (U22B2054), Program for Cheung Kong Scholars and Innovative Research Team in University (IRT_15R53), Fund for Foreign Scholars in University Research and Teaching Programs (the 111 Project) (B07048).

References

- [1] Abdelfatah Ahmed, Divya Velayudhan, Mahmoud ElMezain, Muaz Al Radi, Abderrahmene Boudiaf, Taimur Hassan, Mohamed Deriche, Mohammed Bennamoun, and Naoufel Werghi. Clfs: Clip-driven few-shot learning for baggage threat classification. In *2024 IEEE International Conference on Image Processing (ICIP)*, pages 753–759. IEEE, 2024. 3
- [2] Lukas Bossard, Matthieu Guillaumin, and Luc Van Gool. Food-101-mining discriminative components with random forests. In *Computer vision–ECCV 2014: 13th European conference, zurich, Switzerland, September 6–12, 2014, proceedings, part VI 13*, pages 446–461. Springer, 2014. 6
- [3] Yuhang Cao, Jiaqi Wang, Ying Jin, Tong Wu, Kai Chen, Ziwei Liu, and Dahua Lin. Few-shot object detection via association and discrimination. *Advances in neural information processing systems*, 34:16570–16581, 2021. 2
- [4] Mircea Cimpoi, Subhransu Maji, Iasonas Kokkinos, Sammy Mohamed, and Andrea Vedaldi. Describing textures in the wild. In *Proceedings of the IEEE conference on computer vision and pattern recognition*, pages 3606–3613, 2014. 6
- [5] Jia Deng, Wei Dong, Richard Socher, Li-Jia Li, Kai Li, and Li Fei-Fei. Imagenet: A large-scale hierarchical image database. In *2009 IEEE conference on computer vision and pattern recognition*, pages 248–255. Ieee, 2009. 6
- [6] Alexey Dosovitskiy, Lucas Beyer, Alexander Kolesnikov, Dirk Weissenborn, Xiaohua Zhai, Thomas Unterthiner, Mostafa Dehghani, Matthias Minderer, Georg Heigold, Sylvain Gelly, et al. An image is worth 16x16 words: Transformers for image recognition at scale. *arXiv preprint arXiv:2010.11929*, 2020. 7
- [7] Yaoyang Du, Fang Liu, Licheng Jiao, Zehua Hao, Shuo Li, Xu Liu, and Jing Liu. Augmentative contrastive learning for one-shot object detection. *Neurocomputing*, 513:13–24, 2022. 2
- [8] Li Fei-Fei, Rob Fergus, and Pietro Perona. Learning generative visual models from few training examples: An incremental bayesian approach tested on 101 object categories. In *2004 conference on computer vision and pattern recognition workshop*, pages 178–178. IEEE, 2004. 6
- [9] Peng Gao, Shijie Geng, Renrui Zhang, Teli Ma, Rongyao Fang, Yongfeng Zhang, Hongsheng Li, and Yu Qiao. Clip-adapter: Better vision-language models with feature adapters. *International Journal of Computer Vision*, 132(2):581–595, 2024. 6, 8
- [10] Muhammad Waleed Gondal, Jochen Gast, Inigo Alonso Ruiz, Richard Droste, Tommaso Macri, Suren Kumar, and Luitpold Staudigl. Domain aligned clip for few-shot classification. In *Proceedings of the IEEE/CVF Winter Conference on Applications of Computer Vision*, pages 5721–5730, 2024. 6, 8
- [11] Ziyu Guo, Renrui Zhang, Longtian Qiu, Xianzheng Ma, Xupeng Miao, Xuming He, and Bin Cui. Calip: Zero-shot enhancement of clip with parameter-free attention. In *Proceedings of the AAAI Conference on Artificial Intelligence*, pages 746–754, 2023. 6, 8
- [12] Kaiming He, Xiangyu Zhang, Shaoqing Ren, and Jian Sun. Deep residual learning for image recognition. In *Proceedings of the IEEE conference on computer vision and pattern recognition*, pages 770–778, 2016. 6, 7
- [13] Patrick Helber, Benjamin Bischke, Andreas Dengel, and Damian Borth. Eurosat: A novel dataset and deep learning benchmark for land use and land cover classification. *IEEE Journal of Selected Topics in Applied Earth Observations and Remote Sensing*, 12(7):2217–2226, 2019. 6
- [14] Yunshi Huang, Fereshteh Shakeri, Jose Dolz, Malik Boudiaf, Houda Bahig, and Ismail Ben Ayed. Lp++: A surprisingly strong linear probe for few-shot clip. In *Proceedings of the IEEE/CVF Conference on Computer Vision and Pattern Recognition*, pages 23773–23782, 2024. 6
- [15] Licheng Jiao, Fan Zhang, Fang Liu, Shuyuan Yang, Lingling Li, Zhixi Feng, and Rong Qu. A survey of deep learning-based object detection. *IEEE access*, 7:128837–128868, 2019. 2
- [16] Licheng Jiao, Mengru Ma, Pei He, Xueli Geng, Xu Liu, Fang Liu, Wenping Ma, Shuyuan Yang, Biao Hou, and Xu Tang. Brain-inspired learning, perception, and cognition: A comprehensive review. *IEEE Transactions on Neural Networks and Learning Systems*, 2024. 2
- [17] Licheng Jiao, Xue Song, Chao You, Xu Liu, Lingling Li, Puhua Chen, Xu Tang, Zhixi Feng, Fang Liu, Yuwei Guo, et al. Ai meets physics: a comprehensive survey. *Artificial Intelligence Review*, 57(9):256, 2024. 3
- [18] Licheng Jiao, Mengjiao Wang, Xu Liu, Lingling Li, Fang Liu, Zhixi Feng, Shuyuan Yang, and Biao Hou. Multiscale deep learning for detection and recognition: A comprehensive survey. *IEEE Transactions on Neural Networks and Learning Systems*, 2024. 2
- [19] Muhammad Uzair Khattak, Hanoona Rasheed, Muhammad Maaz, Salman Khan, and Fahad Shahbaz Khan. Maple: Multi-modal prompt learning. In *Proceedings of the IEEE/CVF Conference on Computer Vision and Pattern Recognition*, pages 19113–19122, 2023. 8
- [20] Mona Köhler, Markus Eisenbach, and Horst-Michael Gross. Few-shot object detection: A comprehensive survey. *IEEE Transactions on Neural Networks and Learning Systems*, 2023. 2
- [21] Jonathan Krause, Michael Stark, Jia Deng, and Li Fei-Fei. 3d object representations for fine-grained categorization. In *Proceedings of the IEEE international conference on computer vision workshops*, pages 554–561, 2013. 6
- [22] Dongjun Lee, Seokwon Song, Jihee Suh, Joonmyeong Choi, Sanghyeok Lee, and Hyunwoo J Kim. Read-only prompt optimization for vision-language few-shot learning. In *Proceedings of the IEEE/CVF International Conference on Computer Vision*, pages 1401–1411, 2023. 8
- [23] Janghyeon Lee, Jongsuk Kim, Hyounguk Shon, Bumsoo Kim, Seung Hwan Kim, Honglak Lee, and Junmo Kim. Uni-clip: Unified framework for contrastive language-image pre-training. *Advances in Neural Information Processing Systems*, 35:1008–1019, 2022. 1
- [24] Pengfang Li, Fang Liu, Licheng Jiao, Shuo Li, Lingling Li, Xu Liu, and Xinyan Huang. Knowledge transduction for

- cross-domain few-shot learning. *Pattern Recognition*, 141:109652, 2023. 2
- [25] Shuo Li, Fang Liu, Zehua Hao, Kaibo Zhao, and Licheng Jiao. Unsupervised few-shot image classification by learning features into clustering space. In *European Conference on Computer Vision*, pages 420–436. Springer, 2022. 2
- [26] Shuo Li, Fang Liu, Licheng Jiao, Puhua Chen, and Lingling Li. Self-supervised self-organizing clustering network: A novel unsupervised representation learning method. *IEEE Transactions on Neural Networks and Learning Systems*, pages 1–15, 2022. 3
- [27] Shuo Li, Fang Liu, Licheng Jiao, Puhua Chen, Xu Liu, and Lingling Li. Mfnet: A novel gnn-based multi-level feature network with superpixel priors. *IEEE Transactions on Image Processing*, 31:7306–7321, 2022. 7
- [28] Shuo Li, Fang Liu, Licheng Jiao, Xu Liu, and Puhua Chen. Learning salient feature for salient object detection without labels. *IEEE Transactions on Cybernetics*, 2022. 3
- [29] Shuo Li, Fang Liu, Zehua Hao, Licheng Jiao, Xu Liu, and Yuwei Guo. Minent: Minimum entropy for self-supervised representation learning. *Pattern Recognition*, 138:109364, 2023. 2
- [30] Shuo Li, Fang Liu, Licheng Jiao, Lingling Li, Puhua Chen, Xu Liu, and Wenping Ma. Prompt-based concept learning for few-shot class-incremental learning. *IEEE Transactions on Circuits and Systems for Video Technology*, pages 1–1, 2025. 2
- [31] Yuanchang Liang, Prahlad Vadakkepat, David Kim Huat Chua, Shuyi Wang, Zhigang Li, and Shuxiang Zhang. Recognizing temporary construction site objects using clip-based few-shot learning and multi-modal prototypes. *Automation in Construction*, 165:105542, 2024. 3
- [32] Tsung-Yi Lin, Piotr Dollár, Ross Girshick, Kaiming He, Bharath Hariharan, and Serge Belongie. Feature pyramid networks for object detection. In *Proceedings of the IEEE conference on computer vision and pattern recognition*, pages 2117–2125, 2017. 7
- [33] Mushui Liu, Bozheng Li, and Yunlong Yu. Fully fine-tuned clip models are efficient few-shot learners. *arXiv preprint arXiv:2407.04003*, 2024. 3
- [34] Subhransu Maji, Esa Rahtu, Juho Kannala, Matthew Blaschko, and Andrea Vedaldi. Fine-grained visual classification of aircraft. *arXiv preprint arXiv:1306.5151*, 2013. 6
- [35] Kelly Marchisio, Wei-Yin Ko, Alexandre Bérard, Théo Dehaze, and Sebastian Ruder. Understanding and mitigating language confusion in llms. *arXiv preprint arXiv:2406.20052*, 2024. 1
- [36] Sérgolène Martin, Yunshi Huang, Fereshteh Shakeri, Jean-Christophe Pesquet, and Ismail Ben Ayed. Transductive zero-shot and few-shot clip. In *Proceedings of the IEEE/CVF Conference on Computer Vision and Pattern Recognition*, pages 28816–28826, 2024. 1
- [37] Cristina Menghini, Andrew Delworth, and Stephen Bach. Enhancing clip with clip: Exploring pseudolabeling for limited-label prompt tuning. *Advances in Neural Information Processing Systems*, 36:60984–61007, 2023. 3
- [38] Atsuyuki Miyai, Qing Yu, Go Irie, and Kiyoharu Aizawa. Locoop: Few-shot out-of-distribution detection via prompt learning. *Advances in Neural Information Processing Systems*, 36, 2024. 3
- [39] Maria-Elena Nilsback and Andrew Zisserman. Automated flower classification over a large number of classes. In *2008 Sixth Indian conference on computer vision, graphics & image processing*, pages 722–729. IEEE, 2008. 6
- [40] Kamalesh Palanisamy, Yu-Wei Chao, Xinya Du, Yu Xiang, et al. Proto-clip: Vision-language prototypical network for few-shot learning. *arXiv preprint arXiv:2307.03073*, 2023. 3, 6
- [41] Neal Parikh, Stephen Boyd, et al. Proximal algorithms. *Foundations and trends® in Optimization*, 1(3):127–239, 2014. 6
- [42] Omkar M Parkhi, Andrea Vedaldi, Andrew Zisserman, and CV Jawahar. Cats and dogs. In *2012 IEEE conference on computer vision and pattern recognition*, pages 3498–3505. IEEE, 2012. 6
- [43] Adam Paszke, Sam Gross, Francisco Massa, Adam Lerer, James Bradbury, Gregory Chanan, Trevor Killeen, Zeming Lin, Natalia Gimelshein, Luca Antiga, et al. Pytorch: An imperative style, high-performance deep learning library. *Advances in neural information processing systems*, 32, 2019. 6
- [44] Fang Peng, Xiaoshan Yang, Linhui Xiao, Yaowei Wang, and Changsheng Xu. Sgva-clip: Semantic-guided visual adapting of vision-language models for few-shot image classification. *IEEE Transactions on Multimedia*, 2023. 6
- [45] Farhad Pourpanah, Moloud Abdar, Yuxuan Luo, Xinlei Zhou, Ran Wang, Chee Peng Lim, Xi-Zhao Wang, and QM Jonathan Wu. A review of generalized zero-shot learning methods. *IEEE transactions on pattern analysis and machine intelligence*, 45(4):4051–4070, 2022. 2
- [46] Qi Qian, Yuanhong Xu, and Juhua Hu. Intra-modal proxy learning for zero-shot visual categorization with clip. *Advances in Neural Information Processing Systems*, 36, 2024. 2
- [47] Longtian Qiu, Renrui Zhang, Ziyu Guo, Ziyao Zeng, Zilu Guo, Yafeng Li, and Guannan Zhang. Vt-clip: Enhancing vision-language models with visual-guided texts. *arXiv preprint arXiv:2112.02399*, 2021. 6
- [48] Alec Radford, Jong Wook Kim, Chris Hallacy, Aditya Ramesh, Gabriel Goh, Sandhini Agarwal, Girish Sastry, Amanda Askell, Pamela Mishkin, Jack Clark, et al. Learning transferable visual models from natural language supervision. In *International conference on machine learning*, pages 8748–8763. PMLR, 2021. 1, 2, 3, 6, 8
- [49] Benjamin Recht, Rebecca Roelofs, Ludwig Schmidt, and Vaishaal Shankar. Do imagenet classifiers generalize to imagenet? In *International conference on machine learning*, pages 5389–5400. PMLR, 2019. 6, 7
- [50] Bernardino Romera-Paredes and Philip Torr. An embarrassingly simple approach to zero-shot learning. In *International conference on machine learning*, pages 2152–2161. PMLR, 2015. 2

- [51] Shuai Shao, Yu Bai, Yan Wang, Baodi Liu, and Yicong Zhou. Deil: Direct-and-inverse clip for open-world few-shot learning. In *Proceedings of the IEEE/CVF Conference on Computer Vision and Pattern Recognition*, pages 28505–28514, 2024. 1, 3
- [52] Haoyu Song, Li Dong, Wei-Nan Zhang, Ting Liu, and Furu Wei. Clip models are few-shot learners: Empirical studies on vqa and visual entailment. *arXiv preprint arXiv:2203.07190*, 2022. 3
- [53] Yisheng Song, Ting Wang, Puyu Cai, Subrota K Mondal, and Jyoti Prakash Sahoo. A comprehensive survey of few-shot learning: Evolution, applications, challenges, and opportunities. *ACM Computing Surveys*, 55(13s):1–40, 2023. 2
- [54] K Soomro. Ucf101: A dataset of 101 human actions classes from videos in the wild. *arXiv preprint arXiv:1212.0402*, 2012. 6
- [55] Qianru Sun, Yaoyao Liu, Tat-Seng Chua, and Bernt Schiele. Meta-transfer learning for few-shot learning. In *Proceedings of the IEEE/CVF conference on computer vision and pattern recognition*, pages 403–412, 2019. 2
- [56] Bowen Tang, Jing Zhang, Long Yan, Qian Yu, Lu Sheng, and Dong Xu. Data-free generalized zero-shot learning. In *Proceedings of the AAAI Conference on Artificial Intelligence*, pages 5108–5117, 2024. 2
- [57] Yuwei Tang, Zhenyi Lin, Qilong Wang, Pengfei Zhu, and Qinghua Hu. Amu-tuning: Effective logit bias for clip-based few-shot learning. In *Proceedings of the IEEE/CVF Conference on Computer Vision and Pattern Recognition*, pages 23323–23333, 2024. 2, 3
- [58] Vishaal Uddandarao, Ankush Gupta, and Samuel Albanie. Sus-x: Training-free name-only transfer of vision-language models. In *Proceedings of the IEEE/CVF International Conference on Computer Vision*, pages 2725–2736, 2023. 6
- [59] Vinay Kumar Verma, Gundeep Arora, Ashish Mishra, and Piyush Rai. Generalized zero-shot learning via synthesized examples. In *Proceedings of the IEEE conference on computer vision and pattern recognition*, pages 4281–4289, 2018. 2
- [60] Haohan Wang, Songwei Ge, Zachary Lipton, and Eric P Xing. Learning robust global representations by penalizing local predictive power. *Advances in Neural Information Processing Systems*, 32, 2019. 6, 7
- [61] Hao Wang, Fang Liu, Licheng Jiao, Jiahao Wang, Zehua Hao, Shuo Li, Lingling Li, Puhua Chen, and Xu Liu. Vilt-clip: Video and language tuning clip with multimodal prompt learning and scenario-guided optimization. In *Proceedings of the AAAI Conference on Artificial Intelligence*, pages 5390–5400, 2024. 3
- [62] Zhengbo Wang, Jian Liang, Ran He, Nan Xu, Zilei Wang, and Tieniu Tan. Improving zero-shot generalization for clip with synthesized prompts. In *Proceedings of the IEEE/CVF International Conference on Computer Vision*, pages 3032–3042, 2023. 3
- [63] Guangxing Wu, Junxi Chen, Wentao Zhang, and Ruixuan Wang. Feature adaptation with clip for few-shot classification. In *Proceedings of the 5th ACM International Conference on Multimedia in Asia*, pages 1–7, 2023. 2, 3, 6, 8
- [64] Yongqin Xian, Bernt Schiele, and Zeynep Akata. Zero-shot learning—the good, the bad and the ugly. In *Proceedings of the IEEE conference on computer vision and pattern recognition*, pages 4582–4591, 2017. 2
- [65] Bin Xiao, Haiping Wu, Weijian Xu, Xiyang Dai, Houdong Hu, Yumao Lu, Michael Zeng, Ce Liu, and Lu Yuan. Florence-2: Advancing a unified representation for a variety of vision tasks. In *Proceedings of the IEEE/CVF Conference on Computer Vision and Pattern Recognition*, pages 4818–4829, 2024. 1
- [66] Jianxiong Xiao, James Hays, Krista A Ehinger, Aude Oliva, and Antonio Torralba. Sun database: Large-scale scene recognition from abbey to zoo. In *2010 IEEE computer society conference on computer vision and pattern recognition*, pages 3485–3492. IEEE, 2010. 6
- [67] Xiaohua Zhai, Xiao Wang, Basil Mustafa, Andreas Steiner, Daniel Keysers, Alexander Kolesnikov, and Lucas Beyer. Lit: Zero-shot transfer with locked-image text tuning. In *Proceedings of the IEEE/CVF conference on computer vision and pattern recognition*, pages 18123–18133, 2022. 1
- [68] Jingyi Zhang, Jiaxing Huang, Sheng Jin, and Shijian Lu. Vision-language models for vision tasks: A survey. *IEEE Transactions on Pattern Analysis and Machine Intelligence*, 2024. 1
- [69] Li Zhang, Tao Xiang, and Shaogang Gong. Learning a deep embedding model for zero-shot learning. In *Proceedings of the IEEE conference on computer vision and pattern recognition*, pages 2021–2030, 2017. 2
- [70] Renrui Zhang, Wei Zhang, Rongyao Fang, Peng Gao, Kun-chang Li, Jifeng Dai, Yu Qiao, and Hongsheng Li. Tip-adapter: Training-free adaption of clip for few-shot classification. In *European conference on computer vision*, pages 493–510. Springer, 2022. 1, 3, 6, 8
- [71] Fei Zhou, Peng Wang, Lei Zhang, Wei Wei, and Yanning Zhang. Revisiting prototypical network for cross domain few-shot learning. In *Proceedings of the IEEE/CVF Conference on Computer Vision and Pattern Recognition*, pages 20061–20070, 2023. 2
- [72] Kaiyang Zhou, Jingkang Yang, Chen Change Loy, and Ziwei Liu. Conditional prompt learning for vision-language models. In *Proceedings of the IEEE/CVF conference on computer vision and pattern recognition*, pages 16816–16825, 2022. 2, 8
- [73] Kaiyang Zhou, Jingkang Yang, Chen Change Loy, and Ziwei Liu. Learning to prompt for vision-language models. *International Journal of Computer Vision*, 130(9):2337–2348, 2022. 2, 3, 6, 8
- [74] Ziqin Zhou, Yinjie Lei, Bowen Zhang, Lingqiao Liu, and Yifan Liu. Zegclip: Towards adapting clip for zero-shot semantic segmentation. In *Proceedings of the IEEE/CVF Conference on Computer Vision and Pattern Recognition*, pages 11175–11185, 2023. 2
- [75] Xiangyang Zhu, Renrui Zhang, Bowei He, Aojun Zhou, Dong Wang, Bin Zhao, and Peng Gao. Not all features matter: Enhancing few-shot clip with adaptive prior refinement. In *Proceedings of the IEEE/CVF International Conference on Computer Vision*, pages 2605–2615, 2023. 6, 8